



Funded by the Seventh Framework
Programme of the European Union



Project full title:

Hepatic and Cardiac Toxicity Systems modelling

Project acronym:

HeCaTos

Collaborative project

HEALTH.2013.1.3.-1:

Modelling toxic response in case studies for predictive human safety assessment

FP7-HEALTH-2013-INNOVATION-1-602156-HeCaTos

Deliverable Report D12.1:

Report on initial prediction model

Edited by

Main contributors

Work package 12

Due date of deliverable: M18

Actual submission date: M22

Start date of project: October, 2013

Duration: 60 months

Maastricht University (UM)

Project co-funded by the European Commission within the 7th Framework Programme (2013-2018)		
Dissemination Level		
PU	Public	X
PP	Restricted to other programme participants (including the Commission Services)	
RE	Restricted to a group specified by the consortium (including the Commission Services)	
CO	Confidential, only for members of the consortium (including the Commission Services)	

Contributions to deliverable - Internal review procedure

Deliverable produced by:	Date:
Ralf Herwig - Partner MPIMG	July 27, 2015
Deliverable internally reviewed by:	Date:
Jos Kleijnans - Partner UM	August 17, 2015

Contents

PUBLISHABLE SUMMARY	3
OBJECTIVES	4
INTRODUCTION	4
1. RESULTS	6
1 COMPUTATION OF RELATIVE PATHWAY RESPONSE (RPR) SCORES FROM TOXICOGENOMICS DATA.....	6
1.1 Modelling time-dosage drug treatment data	6
1.2 Pathway concepts.....	8
1.3 RELATIVE PATHWAY RESPONSE SCORES.....	8
1.3.1 Simple case-control case.....	8
1.3.2 Several dosages, multiple time-points – two-factor variance analysis model.....	9
1.3.3 Pathway scoring.....	10
2. PATHWAY INTERACTION NETWORK	11
3. PATHWAY NETWORK MODULE COMPUTATION	13
3.1 BioNet computation of network modules.....	13
3.2 Most affected pathway concepts across human in vitro liver drug treatments	13
3.3 Most affected pathway concepts across rat in vivo heart drug treatments	15
4. USE CASE REPORT: PATHWAY CONCEPTS RELEVANT FOR THE PREDICTION OF DRUG-INDUCED LIVER INJURY (DILI)	16
4.1 Data selection	16
4.1 Training the network.....	19
5. REPOSITORY WITH BENCHMARK DATA (MILESTONE MS27).....	24
5.1 Implementation and availability.....	24
5.2 Drug view.....	24
5.3 STATISTICAL TESTING.....	26
5.4 PATHWAY VIEW	26
SUMMARY	29
DIFFICULTIES	29
REFERENCES	30
ANNEX 1: 119 COMPOUNDS ANALYSED IN HUMAN <i>IN VITRO</i> HEPATOCYTES FROM TG-GATES.....	31
ANNEX 2: 72 COMPOUNDS ANALYSED IN RAT <i>VIVO</i> HEART TISSUE FROM DRUGMATRIX.....	32

The goal of WP12 is to define, conduct and describe use cases for toxicity predictions that are relevant for the work performed in the other WPs. As a first use case we elaborated an approach for pathway-based toxicity prediction. It is anticipated to build an intermediate step from toxicogenomics data analysis (for example the identification of predictive gene expression patterns) to computational modelling by mapping toxicogenomics data onto molecular networks and pathway concepts and by identifying predictive network modules (i.e. initial prediction model) that can serve as the basis for constructing computational models and for defining key molecular events in the design of adverse outcome pathways (AOPs).

To achieve this goal MPIMG and MD have set up a pipeline in WP2 that consists of several steps and that essentially delivers such modules of interacting protein and pathways from toxicogenomics data. In WP12 MPIMG has conducted, as a first use case of HeCaToS, a large data analysis of publicly available toxicogenomics data involving the two publicly available studies TG-GATES and DrugMatrix with a total of 1,152 drug treatment experiments. Data analysis comprised the time-dosage modelling of drug treatment data, the construction of an interaction network derived from pathway concepts, the mapping of the toxicogenomics data onto that network in order to identify most affected pathways and pathway modules. The generated pathway patterns build a resource for associating function and potential phenotypic 'themes' with the drugs under study and might help constructing and improving AOPs for drug action. Furthermore, we demonstrate the usage of such pathway-based analysis with a study on drug-induced liver injury (DILI) and identified a molecular network that is discriminative of DILI severity. Finally, we have built a repository, called ToxDB, that holds these pathway-derived signatures for further research.

OBJECTIVES

The goal of WP12 is to define, conduct and describe use cases for toxicity predictions that are relevant for the work performed in the other WPs. The first use case has elaborated an approach for pathway-based toxicity prediction. It is anticipated to build an intermediate step from toxicogenomics data analysis (for example the identification of predictive gene expression patterns) to computational modelling by mapping toxicogenomics data onto molecular networks and pathway concepts and by identifying predictive network modules (i.e. initial prediction model) that can serve as the basis for constructing computational models and for defining key molecular events in the design of adverse outcome pathways.

INTRODUCTION

In WP2 partners MD and MPIMG have built a pipeline for analysing drug treatment data and for identifying molecular network modules that are predictive for liver and heart toxicity. In WP12 partners MD, MPIMG and UM conducted a use case that elaborated the possibility of pathway-based interpretation of toxicogenomics data in identifying predictive patterns that can be associated with biological function and networks of interacting components. The usefulness of such pathway-based interpretation has been shown previously by us in the context of predicting carcinogenicity of chemical compounds in human *in vitro* assays (Yildirimman et al. (2011) *Toxicol Sci* 124:278-290; Doktorova et al. (2013) *Carcinogenesis* 34:1393-1402).

In this report we describe the usage of pathway concepts for deriving ‘molecular themes’ for drug action prediction. Molecular themes are sets of interacting pathway concepts that can be interpreted as being affected by the corresponding compound in a time-dose dependent manner. To achieve this we implemented the following steps (for each compound):

1. Model experimental gene expression data for each compound by taking into account the full range of time and dose points per experiment; modelling was done with the limma approach;
2. Derive a gene score per compound experiment that indicates whether or not the gene expression has changed upon time and dose axes;
3. For a large number of pre-defined pathways derive a relative pathway response (RPR) score by averaging across all genes assigned to the pathway;
4. Organize the pathways in a graph structure where nodes correspond to pathways and edges between two nodes indicate a significant overlap of the pathway concepts;
5. Weight the nodes in the pathway interaction graph according to the RPR scores computed in point 3; (above);
6. On this weighted graph apply a network algorithm (BioNet) that computes heavy-weighted subnetworks that agglomerate the most significant expression changes.

The result of the analysis is a network module consisting of interacting pathway concepts that is representing the molecular themes with the most significant expression changes.

Since we conducted this analysis for 1,152 compounds from two large publicly available studies (TG-GATES and DrugMatrix) in several biological systems (*in vitro* human hepatocytes, rat tissue etc.) the results provide a repository for emerging molecular themes of drug action and toxicity. Interesting questions covered by the analysis would be, for example, which pathways are in common for many drugs, what are differences according to *in vivo* and *in vitro* systems, according to different tissues and according to different organisms. Since 11 out of 14 hepatotoxic drugs and 6 out of 12 cardiotoxic drugs from the HeCaToS priority lists are covered by this data set, we can use this repository in the further course of the project for anchoring new project omics data as well as initial models on individual drug toxicity.

1. RESULTS

1 Computation of relative pathway response (RPR) scores from toxicogenomics data

The goal of this analysis is to assign each pathway a numerical value (derived from toxicogenomics data) that indicates the response of the pathway with respect to the compound treatment. This essentially done by computing a respective score for each gene and subsequently average over the entire gene group annotated with the pathway.

1.1 Modelling time-dosage drug treatment data

Drug data is typically generated at different doses and response of the cells under study is measured at several time points after drug delivery. In order to cope with this set-up and to identify genes that change over time and dosage it is typically not sufficient to analyse a single time-point/dosage experiment but to take into account changes over time and at several dosages. There are several approaches to the modelling of time-dosage drug data, for example STEM (Ernst and Bar-Joseph (2006) BMC Bioinformatics 7:191) that is mainly a visualization-based clustering approach, Bayesian networks (e.g. Kim et al. (2003) Brief Bioinf 4:228-235) or ANOVA (e.g. Ritchie et al. (2015) Nucleic Acids Res 43:e47).

MPIMG has implemented several ANOVA models using the R/Bioconductor limma package and tested that with all data sets that were made available from DrugMatrix and TG-GATES studies (in total 1,152 experiments). The models tested comprised co-variate factors for time, dosage and time-dosage interaction factor. Five statistical models were considered including parameters for:

- time only;
- dosage only;
- time and dosage;
- time-dosage interaction factor only;
- full model consisting of time, dosage and time-dosage interaction factor.

Fig. 1 gives an overall overview on the processed data sets. Fig. 1A displays the five models with respect to the number of dosage and time-points. As can be seen from the 1,152 experiments approx. 50% are available at three dosages and at least three time-points ($179+344=523$). The Y-axes display the numbers of differentially expressed genes with respect to the different models. Since these numbers are FDR corrected, they could serve as an indicator for the sensitivity of the model and it can be seen that in most cases the full model consisting of time, dosage and interaction factor as model parameters is the most sensitive. Thus, we kept this model for further analysis.

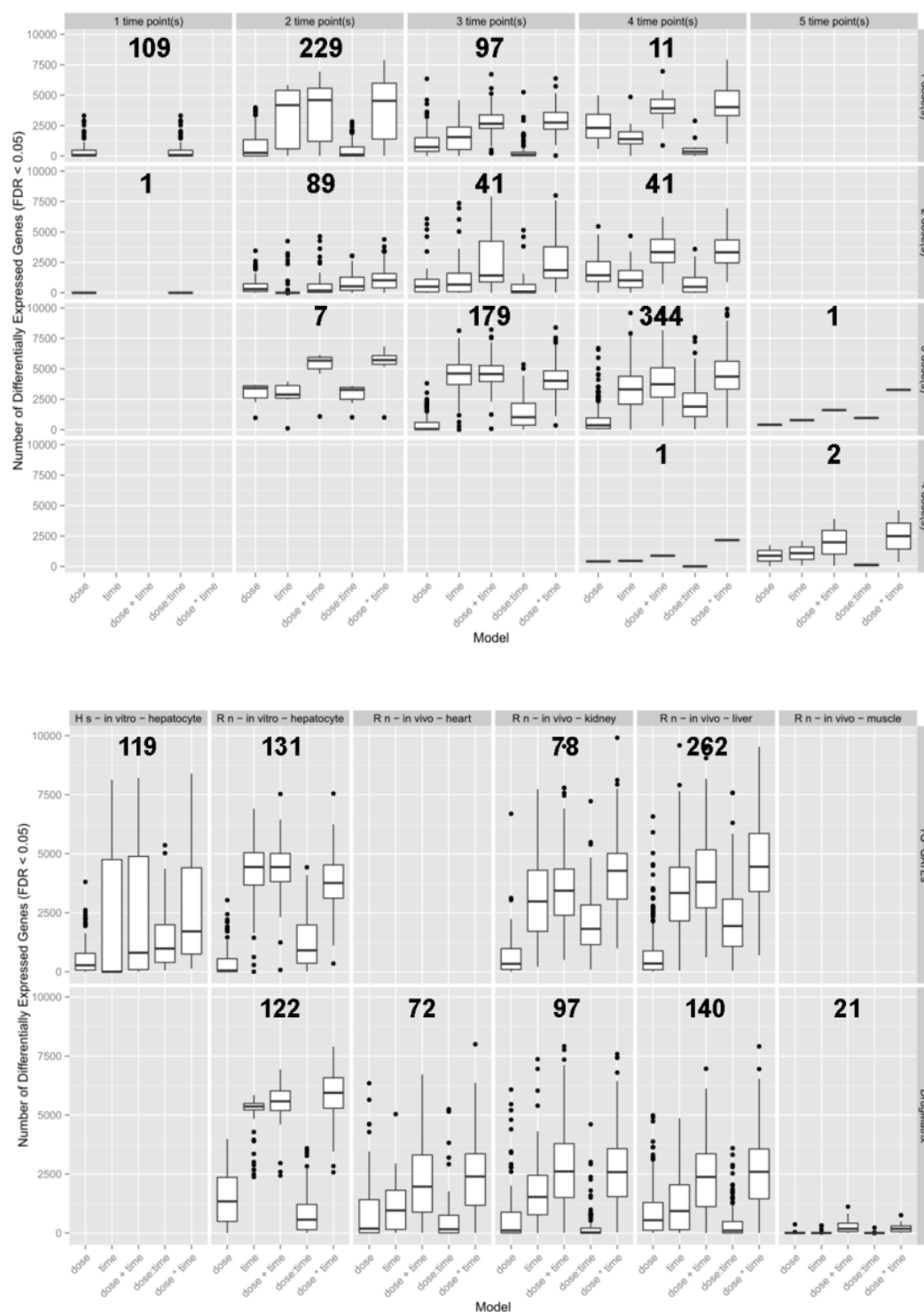


Figure 1: ANOVA models tested with TG-GATES and DrugMatrix data. X-axes describe the five models under consideration: dose – dosage factor only; time – time factor only; dose+time - time and dosage factor; dose:time - interaction factor only; dose*time - full model. Box plots represent number of differentially expressed genes after FDR correction. A) Experiments with respect to time and dose points. B) Experiments with respect to the biological material under consideration.

1.2 Pathway concepts

The pathway concepts, i.e. the assignments of genes to functional groups, are derived from MPIMG's ConsensusPathDB resource (<http://consensuspathdb.org>). It agglomerates 4,349 pathway concepts from the following resources:

- BioCarta;
- EHMN;
- HumanCyc;
- INOH;
- KEGG;
- NetPath;
- PID;
- PharmGKB;
- Reactome;
- SMPDB;
- Signalink;
- Wikipathways.

1.3 Relative pathway response scores

The purpose of the relative pathway response (RPR) scoring is to assign each pathway a numerical value that quantifies its response measured with omics data. Although we predominantly work with gene expression data, however, in principle there is no restriction to this type of data and experimental values could be any quantitative read-out from transcriptomics or proteomics.

A pathway $path_k$ of size n is defined as a set of genes $M_k = \{g_1, \dots, g_n\}$ of size $|M_k| = n$. Gene lists are derived from the ConsensusPathDB since it summarizes the main publicly available pathway resources.

1.3.1 Simple case-control case

Suppose genome-wide case-control experiments are carried out with some material, e.g. human tissue, rat tissue and/or cell lines, including replicates. In the simplest case such experiments consist of a chemical treatment of the cells at a certain dosage which are compared against the untreated control cells at a matched time point after delivery of the chemical. This yields for each gene g_i and each chemical j , a fold-change r_{ij} and P-value p_{ij} according to a suitable statistical test procedure (e.g. Student's t-test, Wilcoxon's rank test, edgeR and others). The test could be any procedure that judges the significance of the fold-change given the null hypothesis of no change of expression.

We now compute a gene score s_{ij} for gene g_i and chemical j by:

$$s_{ij} = |\log_2 r_{ij}| |\log_{10} p_{ij}|.$$

The gene score describes a weighted fold-change of the gene with respect to the particular treatment, where the weight is increasing with the significance of the fold-change.

1.3.2 Several dosages, multiple time-points – two-factor variance analysis model

In a more complicated set up (cf. point 1.1 above), the chemical is given at different dosages and response is measured at different time points after delivery. In such a case, for each gene g_i and chemical j we can model the response with a (two-factor) variance analysis model and derive a gene score that indicates the time- and dose-related effects of the compound on the individual gene expression.

In the two studies used (TG-GATES and DrugMatrix), each individual treatment experiment consists of one to four different time points $x_t, 1 \leq t \leq 4$ and one to five different concentration levels $x_c, 1 \leq c \leq 5$. Treatment experiments were replicated two to three times for drug treatments and up to ten times for controls. Controls are time series experiments without application of a drug.

The gene expression response of gene g_i to compound j was estimated using a variance analysis model with the following terms:

$$y_{ij} = X\beta_{ij} + \varepsilon_{ij}, \text{ where}$$

y_{ij} is the vector with the experimental data.

$$X = \begin{pmatrix} 1 & x_{t=1} & x_{c=1} & x_{t=1}x_{c=1} \\ 1 & x_{t=2} & x_{c=1} & x_{t=2}x_{c=1} \\ \vdots & \vdots & \vdots & \vdots \\ 1 & x_{t=t} & x_{c=c} & x_{t=t}x_{c=c} \end{pmatrix} \text{ is the design matrix of all existing combinations of time and dosage}$$

points that models the linear response of each gene to the time variable, the dosage variable and their interaction.

$$\beta_{ij} = \begin{pmatrix} \beta_{ij1} \\ \beta_{ijt} \\ \beta_{ijc} \\ \beta_{ijtc} \end{pmatrix} \text{ is the vector of model coefficients, and } \varepsilon_{ij} \text{ is a Gaussian noise term.}$$

Computation was done with the help of the R/Bioconductor package *limma* given the expression vectors for a specific treatment and the corresponding design matrix. This yields an estimator, $\hat{\beta}_{ij}$, for each gene g_i drug treatment j of the model parameter vector β_{ij} .

Using the experimental treatment data for each gene g_i and each chemical j , we estimate coefficients and derive an F-test P-value (adjusted for multiple testing) in order to compute a gene score s_{ij} in analogy to the simple case-control case described above. The score for each gene is defined as the absolute value of the \log_2 of the Euclidean norm of the estimated coefficients (without the intercept) times the \log_{10} of the adjusted p-value:

$$s_{ij} = \left| \log_2 \sqrt{\hat{\beta}_{ijt}^2 + \hat{\beta}_{ijc}^2 + \hat{\beta}_{ijtc}^2} \right| \left| \log_{10} p_{ij} \right| .$$

That means, the strength of the response given by the estimated coefficients is weighted by the P-value. The directionality of the response is not maintained.

1.3.3 Pathway scoring

The goal is to assign each pathway a numerical score that indicates the effect of the compound on the pathway. Once the gene scores are computed (either for the simple case-control or the multiple time-dose model), we can assign each pathway a pathway score, $path_{kj}$, for pathway $path_k$ and chemical j as the average gene score of all genes assigned to the pathway:

$$path_{kj} = \frac{1}{|M_k|} \sum_{g_i \in M_k} s_{ij}.$$

In order to make pathway scores comparable across different treatments, we finally divide each pathway score derived from a particular treatment by the median pathway score over all pathways with respect to the treatment, $path_{ij}$, and compute the relative response score (RPR):

$$RPR_{kj} = \log_2 \left(\frac{path_{kj}}{\text{median}(path_{ij}|i)} \right).$$

The consequence of the transformation is that in all treatments half of the pathways get negative RPRs and half of them get positive ones. RPRs are comparable across different treatments and follow a Gaussian distribution (Fig. 2A). Thus, higher RPRs reflect significant pathway responses to the chemical treatment. Furthermore, RPRs reflect the strength of chemical dose (see Fig. 1B) which is a necessary condition when quantifying pathway responses.

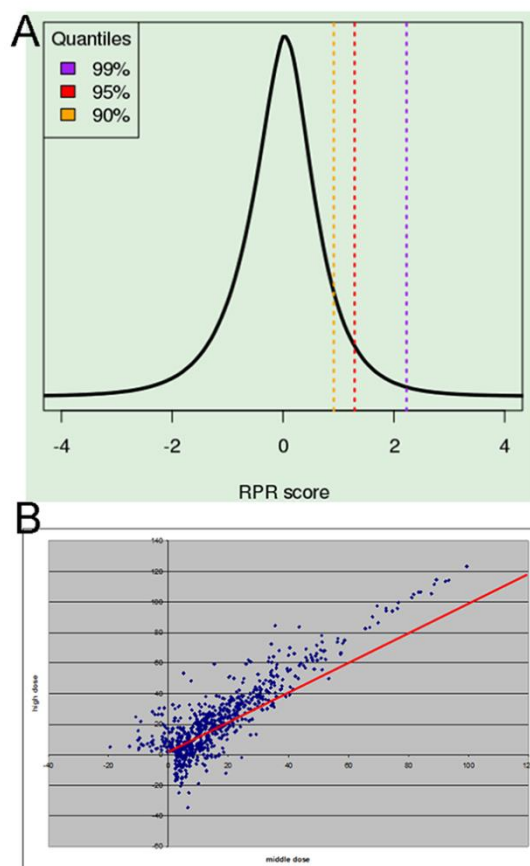


Figure 2: A) The relative pathway response (RPR) scores are Gaussian-distributed and comparable across different compound treatment experiments; vertical lines correspond to the 90th, 95th and 99th quantile of the distribution. **B)** RPR scores reflect chemical dose. Scores derived from ‘middle’ (X-axis) and ‘high’ (Y-axis) doses for responding pathways across different treatments increase with dosage. Red line: similar response.

2. Pathway interaction network

In order to derive a pathway interaction network we generated a graph structure where each node corresponds to a pathway. In order to eliminate pathway concepts that are very specific we took into account only those with more than five members (i.e. genes/proteins associated with the pathway). For two pathways we evaluated the overlap of the corresponding gene lists with Fisher’s exact test and an interaction is drawn between two pathways if the corrected P-value of the test is $< 10^{-4}$ using Bonferroni correction. This results in a network consisting of 3,216 nodes and 96,794 edges.

Fig. 3 displays the resulting network. As can be seen there is basically one large connected component which means that most pathways are interconnected with each other. The network contains nodes (pathways) with overlap to many other pathways (maximum: 589) as well as nodes with smaller overlap (minimum: 5). The average node degree is 60 and the connectivity index (a measure that indicates how neighbourhoods of genes are connected ranging between 0 and 1) is relatively high (0.71). The node degree follows a power law distribution which is typical for biological networks (Fig. 3).

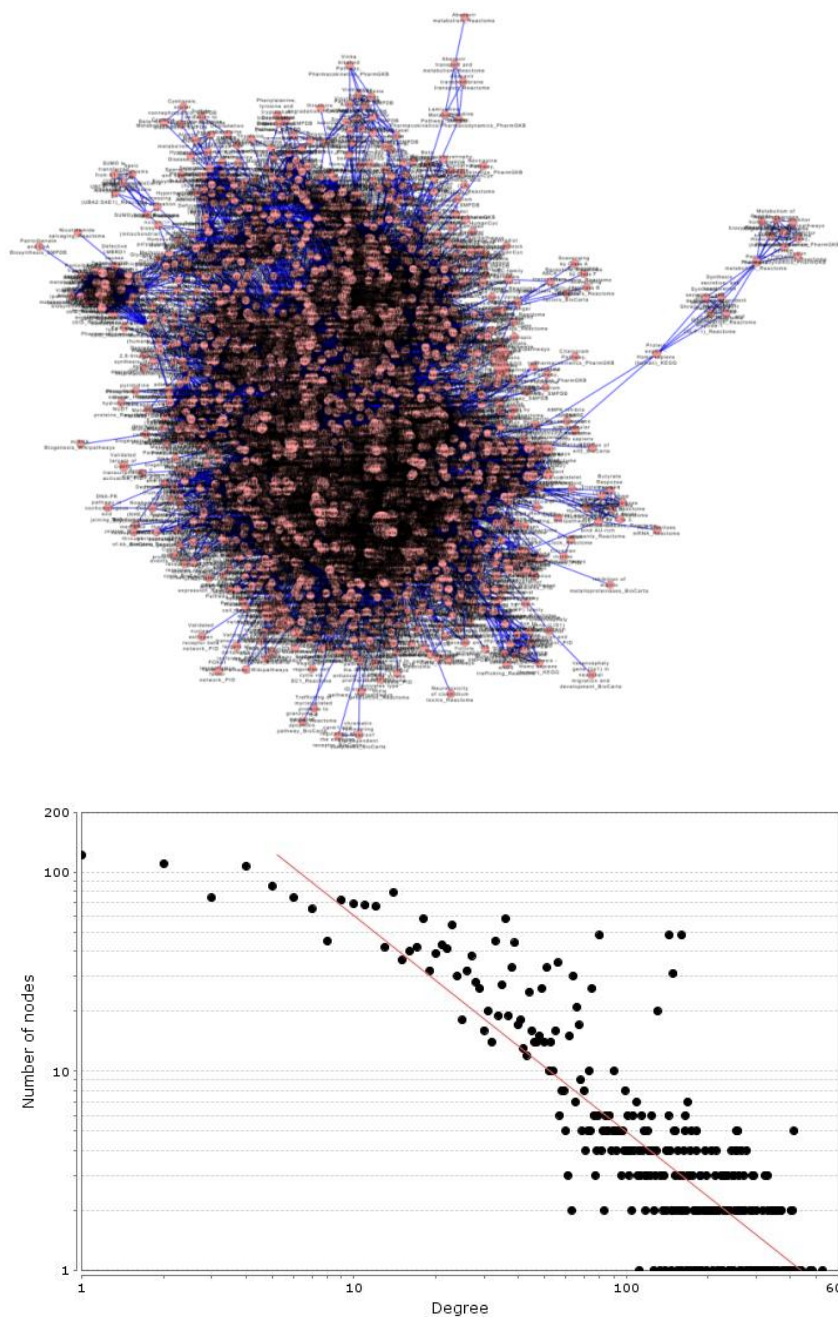


Figure 3: Top: Interaction graph derived from the pathway concepts. **Bottom:** Node degree distribution, y , follows a power law $y = ax^b$ with $a = 726.5$ and $b = -1.082$. The R^2 fit is $R^2 = 0.77$.

3. Pathway network module computation

Here, we investigated what parts of the network are most responsive to an individual drug as well as across many different drugs. This goal was achieved by applying a graph algorithm to the pathway interaction network described in point 2 above. Experimental response data was taken into account by weighting the nodes (pathways) according to their response measured with the full ANOVA model described in point 1.3 above. Thus, if a node gets a high weight this corresponds to a high response of the corresponding pathway across time or dose (or both factors) measured by the microarray data and vice versa. The graph algorithm then computes heavy-weighted subnetworks that agglomerate much of the measured pathway responses, and these subnetworks are likely candidates for predictive models and functional experiments.

3.1 BioNet computation of network modules

We used the interaction network described in point 2 above and the pathway scores described in point 1.3. Next we applied the BioNet algorithm that is available as an R/Bioconductor package. The algorithm is part of the implemented pipeline described in Deliverable 2.3 and has extensively been described in Deliverable 2.1 in the first reporting period.

The BioNet algorithm yields for each drug a network module computed from the weighted pathway interaction network that can be interpreted as the most affected part of the network for each drug and thus serves as a network-based predictor of drug toxicity.

3.2 Most affected pathway concepts across human in vitro liver drug treatments

We analysed all experiments from human hepatocytes that are made available by TG-GATES. This corresponds to 119 drug experiments (cf. Fig. 1). A list of compounds is given in Annex 1 of this report. For each compound the graph nodes are weighted individually by the corresponding RPR scores and the graph algorithm computes a heavy-weighted network module consisting of a set of nodes (pathways). An immediate question is whether there is some commonality in the computed subgraphs across the 119 drugs examined. Indeed, the overlap in pathway concepts is fairly strong and some common molecular themes can be observed.

Molecular themes found predominantly in the computed network modules of many of the drugs are e.g. lipid metabolism (70 out of 119 drugs), PPAR signalling (56), cholesterol biosynthesis (71). Table 1 lists the 30 most common pathways that have been identified in the respective network modules of the 119 drugs.

Pathway	Database	Hits
cholesterol.biosynthesis	HumanCyc	71
Metabolism.of.lipids.and.lipoproteins	Reactome	70
Cholesterol.Biosynthesis	Wikipathways	67
Synthesis.of.Prostaglandins..PG..and.Thromboxanes..TX	Reactome	67
Oxidative.Stress.Regulatory.Pathway..Erythrocyte	PharmGKB	67
Pentose.and.glucuronate.interconversions	KEGG	56
PPAR.alpha.pathway	Wikipathways	56
sphingosine.and.sphingosine.1.phosphate.metabolism	HumanCyc	56
Cholesterol.biosynthesis	Reactome	55
acetone.degradation.l..to.methylglyoxal	HumanCyc	55
Oxidative.Stress	Wikipathways	54
Chylomicron.mediated.lipid.transport	Reactome	54
HDL.mediated.lipid.transport	Reactome	54
Fatty.Acids.Omega.Oxidation	Wikipathways	54
Detoxification.of.Reactive.Oxygen.Species	Reactome	51
Hypercholesterolemia	SMPDB	51
Steroid.Biosynthesis	SMPDB	51
superpathway.of.cholesterol.biosynthesis	HumanCyc	49
reactive.oxygen.species.degradation	HumanCyc	46
Vitamin.B12.Metabolism	Wikipathways	46
Benzodiazepine.Pathway..Pharmacokinetics	PharmGKB	45
allopregnanolone.biosynthesis	HumanCyc	45
Steroid.hormone.biosynthesis	KEGG	45
Mono.unsaturated.fatty.acid.beta.oxidation	EHMN	44
Steroid.biosynthesis	KEGG	44
Mitochondrial.Beta.Oxidation.of.Long.Chain.Saturated.Fatty.Acids	SMPDB	44
Folate.Metabolism	Wikipathways	43
Glutathione.metabolism	Wikipathways	42
Mitochondrial.Beta.Oxidation.of.Medium.Chain.Saturated.Fatty.Acids	SMPDB	42
Fatty.Acids.Elongation.In.Mitochondria	SMPDB	42

Table 1. Pathway concepts found predominantly affected by 119 drugs in human in vitro hepatocytes. Database: annotation source for pathway concept; Hits: number of times that this pathway concept has been found in a network module computed from the pathway interaction graph (maximum = 119).

The network modules computed from the different compounds varied greatly in size. The largest module comprising 132 pathways was computed for theophylline, while the smallest modules was computed for ethinylestradiol and contained 31 pathways. However, it should be noted that these numbers do not refer to different pathways because the corresponding gene lists are largely overlapping.

The results point already to very important hallmarks of drug toxicity such as mitochondrial damage as well as to important nuclear receptor signalling pathways such as PPAR alpha. Mitochondrial

dysfunction is a generic term and manifests through several metabolic pathways and damage of different mitochondrial components. Pathways that have been associated with mitochondrial dysfunction are oxidative stress, energy shortage, among others, and a key hallmark is the inhibition of mitochondrial fatty acid oxidation what can lead to steatosis and ultimately to steatohepatitis and liver failure. PPAR alpha is known as a key regulator of mitochondrial (and also peroxisomal) fatty acid oxidation (Begriche et al. (2011) J Hepatology 54:773-794).

Thus, the identified most common network modules already point to key molecular pathways of liver toxicity and will be further explored during the course of the project.

3.3 Most affected pathway concepts across rat *in vivo* heart drug treatments

In a second approach we analysed all data that was made available for heart tissue in the two studies. Unfortunately, no human data is given so we had to concentrate on rat *in vivo* heart data from DrugMatrix resource. In order to map rat expression data onto human pathways we had to perform an intermediate step of homology assignment: Rat gene identifiers were mapped to human gene identifiers in a one-to-many way and corresponding experimental data was assigned to the human genes in order to compute the gene- and pathway scores described in section 1. Data contained 72 drugs (cf. Fig. 1), a list of compounds is given in Annex 2.

Similar to the previous section we observe strong overlap of pathway concepts across the different drugs. Molecular themes found predominantly in the computed network modules are e.g. TCA cycle (63 out of 72 drugs), respiratory electron transport (63) and muscle contraction (60), oxidative phosphorylation (61). Table 2 lists the 30 most common pathways that have been identified in the respective network modules of the 72 drugs.

Pathway	Database	Hits
The.citric.acid..TCA..cycle.and.respiratory.electron.transport	Reactome	63
Electron.Transport.Chain	Wikipathways	63
Respiratory.electron.transport	Reactome	62
Oxidative.phosphorylation	Wikipathways	61
Oxidative.phosphorylation	KEGG	60
Cardiac.muscle.contraction	KEGG	60
Citrate.cycle..TCA.cycle	KEGG	58
Citric.acid.cycle..TCA.cycle	Reactome	58
Mitochondrial.Electron.Transport.Chain	SMPDB	58
Formation.of.ATP.by.chemiosmotic.coupling	Reactome	58
TCA.Cycle	Wikipathways	57
Pyruvate.metabolism.and.Citric.Acids..TCA..cycle	Reactome	57
Striated.Muscle.Contraction	Wikipathways	56
X2.ketoglutarate.dehydrogenase.complex.deficiency	SMPDB	56
Citric.Acids.Cycle	SMPDB	56
Congenital.lactic.acidosis	SMPDB	56
Fumarate.deficiency	SMPDB	56

Mitochondrial.complex.II.deficiency	SMPDB	56
Pyruvate.dehydrogenase.deficiency	SMPDB	56
TCA.cycle	HumanCyc	56
Striated.Muscle.Contraction	Reactome	53
superpathway.of.conversion.of.glucose.to.acetyl.CoA.and.entry.into.the.TCA.cycle	HumanCyc	52
TCA.cycle	EHMN	50
Transfer.of.Acetyl.Groups.into.Mitochondria	SMPDB	49
Mitochondrial.Beta.Oxidation.of.Medium.Chain.Saturated.Fatty.Acids	SMPDB	44
mitochondrial.fatty.acid.beta.oxidation.of.saturated.fatty.acids	Reactome	44
Muscle.contraction	Reactome	44
Carnitine.palmitoyl.transferase.deficiency	SMPDB	43
Fatty.acid.Metabolism	SMPDB	43
Long.chain.acyl.CoA.dehydrogenase.deficiency..LCAD	SMPDB	43

Table 2. Pathway concepts found predominantly affected by 72 drugs in rat in vitro heart tissue. Database: annotation source for pathway concept; Hits: number of times that this pathway concept has been found in a network module computed from the pathway interaction graph (maximum = 72).

The results observed are well in agreement with literature knowledge on cardiotoxicity. For example, ‘*oxidative phosphorylation*’ is altered by 61 out of 72 drugs. It has been shown by proteomics analysis that for example anthracyclines (such as doxorubicin, idarubicin, 4'-epidoxorubicin, daunorubicin) cause changes in proteins crucial for oxidative phosphorylation (Sterba et al. (2011) J Mol Cell Cardiol 50:849-862). All of the four compounds show strong response with respect to various annotations of ‘*oxidative phosphorylation*’. Additionally, it is observable from the toxicogenomics data that cardiotoxic drugs alter energy production – one of the main functions of mitochondria (Finsterer and Ohnsorge (2013) Regul Toxicol Pharmacol 67:434-445). This manifests in the dominant response themes ‘*citric cycle*’ and ‘*TCA cycle*’ found in 50-63 out of 72 drugs dependent on the respective database annotation.

4. Use case report: Pathway concepts relevant for the prediction of drug-induced liver injury (DILI)

While the experiments in the previous section used pathway scores derived from multiple time and dosage experiments per drug and give an overview of the entire drug panel as a resource for functional mapping of drug action, we further examined whether we can derive meaningful molecular themes by simple case-control studies in a more detailed manner, in particular to describe DILI hazard of compounds. Thus, we focused on pathway scores computed from the simple model (point 1.2) and a subset of experimental data for which DILI effects have been well documented what will be described in this section.

4.1 Data selection

Together with partners UM and MD, MPIMG performed a survey of available suitable human liver data sets from the TG-GATES study. We identified human *in vitro* hepatocyte expression data for 61

compounds that were additionally examined by the FDA according to their DILI risk using intensive literature mining and reading of box warnings (Chen et al., 2011). The compounds are listed in Table 3.

DrugName (CEL)	ChEMBL ID	CAS	SeverityClass	DILICConcern
Simvastatin	CHEMBL1064	79902-63-9	3	Less-DILI-Concern
Colchicine	CHEMBL107	64-86-8	6	Less-DILI-Concern
Diazepam	CHEMBL12	439-14-5	4	Less-DILI-Concern
Methyltestosterone	CHEMBL1395	58-18-4	2	Less-DILI-Concern
Penicillamine	CHEMBL1430	52-67-5	2	Less-DILI-Concern
Tetracycline	CHEMBL1440	60-54-8	2	Less-DILI-Concern
Ethionamide	CHEMBL1441	536-33-4	3	Less-DILI-Concern
Omeprazole	CHEMBL1503	73590-58-6	4	Less-DILI-Concern
Naproxen	CHEMBL154	22204-53-1	3	Less-DILI-Concern
Azathioprine	CHEMBL1542	446-86-6	3	Less-DILI-Concern
Captopril	CHEMBL1560	62571-86-2	6	Less-DILI-Concern
Nifedipine	CHEMBL193	21829-25-4	3	Less-DILI-Concern
Cimetidine	CHEMBL30	51481-61-9	2	Less-DILI-Concern
Furosemide	CHEMBL35	54-31-9	2	Less-DILI-Concern
Phenobarbital	CHEMBL40	50-06-6	3	Less-DILI-Concern
Etoposide	CHEMBL44657	33419-42-0	3	Less-DILI-Concern
Gemfibrozil	CHEMBL457	25812-30-0	3	Less-DILI-Concern
Glibenclamide	CHEMBL472	10238-21-8	3	Less-DILI-Concern
Thioridazine	CHEMBL479	50-52-2	5	Less-DILI-Concern
Chlorpropamide	CHEMBL498	94-20-2	2	Less-DILI-Concern
Ranitidine	CHEMBL512	66357-35-5	5	Less-DILI-Concern
Lomustine	CHEMBL514	13010-47-4	3	Less-DILI-Concern
Disopyramide	CHEMBL517	05.09.3737	2	Less-DILI-Concern
Ibuprofen	CHEMBL521	15687-27-1	3	Less-DILI-Concern
Haloperidol	CHEMBL54	52-86-8	5	Less-DILI-Concern
Clofibrate	CHEMBL565	637-07-0	3	Less-DILI-Concern
Triamterene	CHEMBL585	396-01-0	5	Less-DILI-Concern
Meloxicam	CHEMBL599	71125-38-7	3	Less-DILI-Concern
Promethazine	CHEMBL643	60-87-7	5	Less-DILI-Concern
Triazolam	CHEMBL646	28911-01-5	4	Less-DILI-Concern
Fenofibrate	CHEMBL672	49562-28-9	3	Less-DILI-Concern
Mefenamic acid	CHEMBL686	61-68-7	3	Less-DILI-Concern
Chlorpromazine	CHEMBL71	50-53-3	2	Less-DILI-Concern
Tolbutamide	CHEMBL782	64-77-7	2	Less-DILI-Concern
Cyclophosphamide	CHEMBL88	50-18-0	5	Less-DILI-Concern
Famotidine	CHEMBL902	76824-35-6	3	Less-DILI-Concern
Carbamazepine	CHEMBL108	298-46-4	7	Most-DILI-Concern
Valproic acid	CHEMBL109	99-66-1	8	Most-DILI-Concern
Acetaminophen	CHEMBL112	103-90-2	5	Most-DILI-Concern
Chlormezanone	CHEMBL1200714	80-77-3		Most-DILI-Concern

Dantrolene	CHEMBL1201288	7261-97-4	8	Most-DILI-Concern
Danazol	CHEMBL1479	17230-88-5	8	Most-DILI-Concern
Methimazole	CHEMBL1515	60-56-0	8	Most-DILI-Concern
Propylthiouracil	CHEMBL1518	51-52-5	8	Most-DILI-Concern
Sulindac	CHEMBL15770	38194-50-2	8	Most-DILI-Concern
Phenytoin	CHEMBL16	57-41-0	8	Most-DILI-Concern
Acetazolamide	CHEMBL20	59-66-5	8	Most-DILI-Concern
Diltiazem	CHEMBL23	42399-41-7	4	Most-DILI-Concern
Sulfasalazine	CHEMBL421	599-79-1	5	Most-DILI-Concern
Methyldopa	CHEMBL459	555-30-6	8	Most-DILI-Concern
Griseofulvin	CHEMBL562	126-07-8	8	Most-DILI-Concern
Nitrofurantoin	CHEMBL572	67-20-9	8	Most-DILI-Concern
Indomethacin	CHEMBL6	53-86-1	5	Most-DILI-Concern
Amiodarone	CHEMBL633	1951-25-3	8	Most-DILI-Concern
Isoniazid	CHEMBL64	54-85-3	8	Most-DILI-Concern
Trimethadione	CHEMBL695	127-48-0	5	Most-DILI-Concern
Ciprofloxacin	CHEMBL8	85721-33-1	7	Most-DILI-Concern
Flutamide	CHEMBL806	13311-84-7	8	Most-DILI-Concern
Terbinafine	CHEMBL822	91161-71-6	8	Most-DILI-Concern
Disulfiram	CHEMBL964	97-77-8	8	Most-DILI-Concern
Allopurinol	CHEMBL1467	315-30-0	8	Most-DILI-Concern

Table 3: Compounds for which DILI classification (columns 4 and 5) and human *in vitro* expression data is available.

36 compounds were assigned a ‘*Less-DILI*’ risk whereas 25 compounds were assigned a ‘*Most-DILI*’ risk. Furthermore, we added a second classification based on structure-activity relationships (SARs; Greene et al., 2010). This classification judges the compounds according to ‘*no evidence*’ (NE), ‘*weak evidence for human hepatotoxicity*’ (WE), ‘*animal hepatotoxicity*’ (AH) and ‘*human hepatotoxicity*’ (HH).

The purpose of cross-validating different annotation systems was to retrieve an initial classification with strong evidence. As it can be seen from Fig. 4 there is a considerable overlap with both classification systems with the ‘*Most-DILI*’ assigned compounds while there is less agreement with the ‘*Less-DILI*’ assigned compounds. Of the 36 ‘*Less-DILI*’ compounds only 6 had the assignment WE and 13 had the assignment HH indicating a conflicting result. This might pose a problem for the training process and lead to ambiguous classifiers. 17 of the compounds were not investigated with the SAR approach. In contrast, the classification of the ‘*Most-DILI*’ compounds was mostly in agreement with the SAR classification: 18 out of 25 compounds were classified as HH with 7 compounds that were not under investigation.

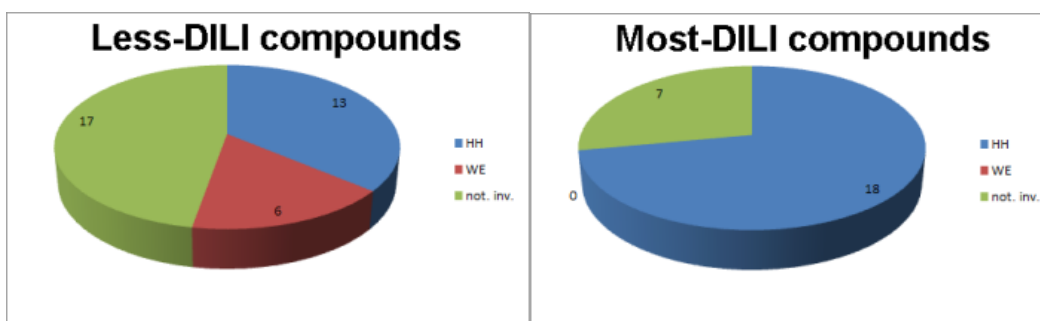


Figure 4: Overlap of two different annotation approaches for human drug hepatotoxicity.

For constructing the predictive network we decided to use those compounds as training compounds that have a high overlap in annotation, namely 6 compounds with ‘*Less-DILI*’ AND ‘*WE*’ annotation on the one hand and 18 compounds with ‘*Most-DILI*’ AND ‘*HH*’ annotation on the other hand.

4.1 Training the network

We computed relative pathway response scores as described in point 1.3 above for all 24 training compounds for all 4,078 pathways available in ConsensusPathDB. Next we used Student’s t-test on the relative response pathway scores in order to identify discriminating pathways. In total, 115 pathways were identified that are discriminating the two compound groups. The discrimination was perfect which was visualized with principal component analysis (Fig. 5) and hierarchical clustering (Fig. 6). Table 4 lists the top-discriminating pathways with P-value <0.01.

Pathway	TTEST P-value
hiv-1 nef: negative effector of fas and tnfr_BioCarta	2,41862E-05
ATM pathway_PID	3,56627E-05
Disease_Reactome	7,84365E-05
Eicosanoid Synthesis_Wikipathways	0,000377635
activation of csk by camp-dependent protein kinase inhibits signaling through the t cell receptor_BioCarta	0,000940673
LDL-mediated lipid transport_Reactome	0,001667597
Packaging Of Telomere Ends_Reactome	0,001871064
Crosslinking of collagen fibrils_Reactome	0,001944483
Prostaglandin Synthesis and Regulation_Wikipathways	0,002117497
Transcription_Reactome	0,002121459
Wnt_NetPath	0,003489862
Oxidative Stress Induced Senescence_Reactome	0,003828279
Constitutive Signaling by NOTCH1 PEST Domain Mutants_Reactome	0,003850705
Homologous recombination - Homo sapiens (human)_KEGG	0,004163002
Epstein-Barr virus infection - Homo sapiens (human)_KEGG	0,004506583
roles of arrestin dependent recruitment of src kinases in gpqr signaling_BioCarta	0,005024172
Acyl chain remodelling of PS_Reactome	0,00595682
proteasome complex_BioCarta	0,006851791

chrebp regulation by carbohydrates and camp_BioCarta	0,006874307
alpha-Linolenic acid metabolism - Homo sapiens (human)_KEGG	0,006996614
Abacavir transmembrane transport_Reactome	0,007785033
Angiogenesis overview_Wikipathways	0,007897658
tumor suppressor arf inhibits ribosomal biogenesis_BioCarta	0,008248802
Constitutive Signaling by NOTCH1 HD Domain Mutants_Reactome	0,008503588
Influenza A - Homo sapiens (human)_KEGG	0,008872292
Extrinsic Pathway for Apoptosis_Reactome	0,009189908
Ceramide signaling pathway_PID	0,009898303

Table 4: Top-discriminating pathways (P-value<0.01) for DILI risk.

As can already be seen from this short list the derived pathway concepts illustrate important molecular hallmarks of hepatotoxicity such as apoptosis, mitochondrial (dys-)function, stress responses as well as immune reactions.

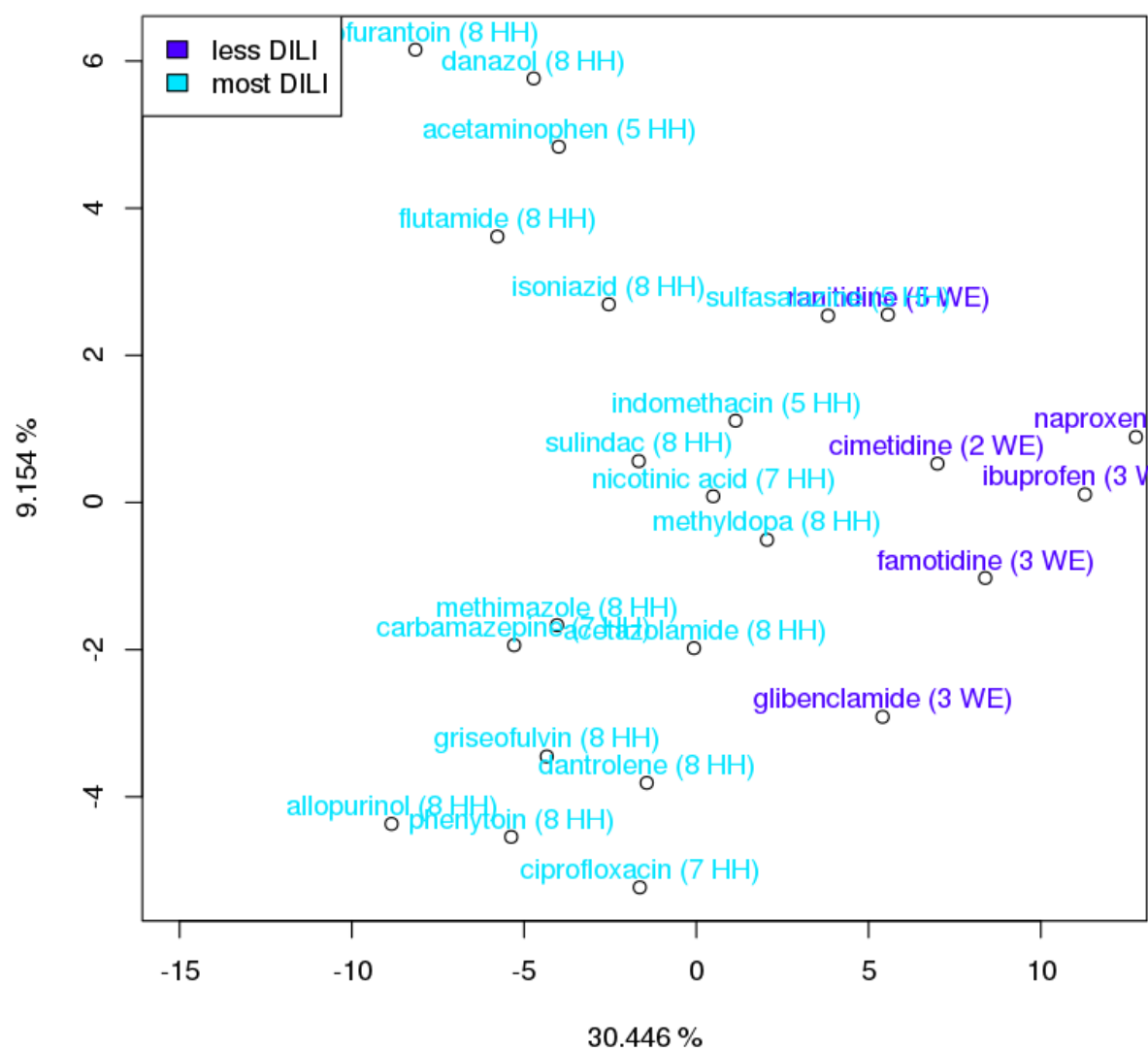


Figure 5: PCA of compounds based on the relative pathway response (RPR) scores for 115 pathways. Both axes explain approx. 40% of the variance in the data set.

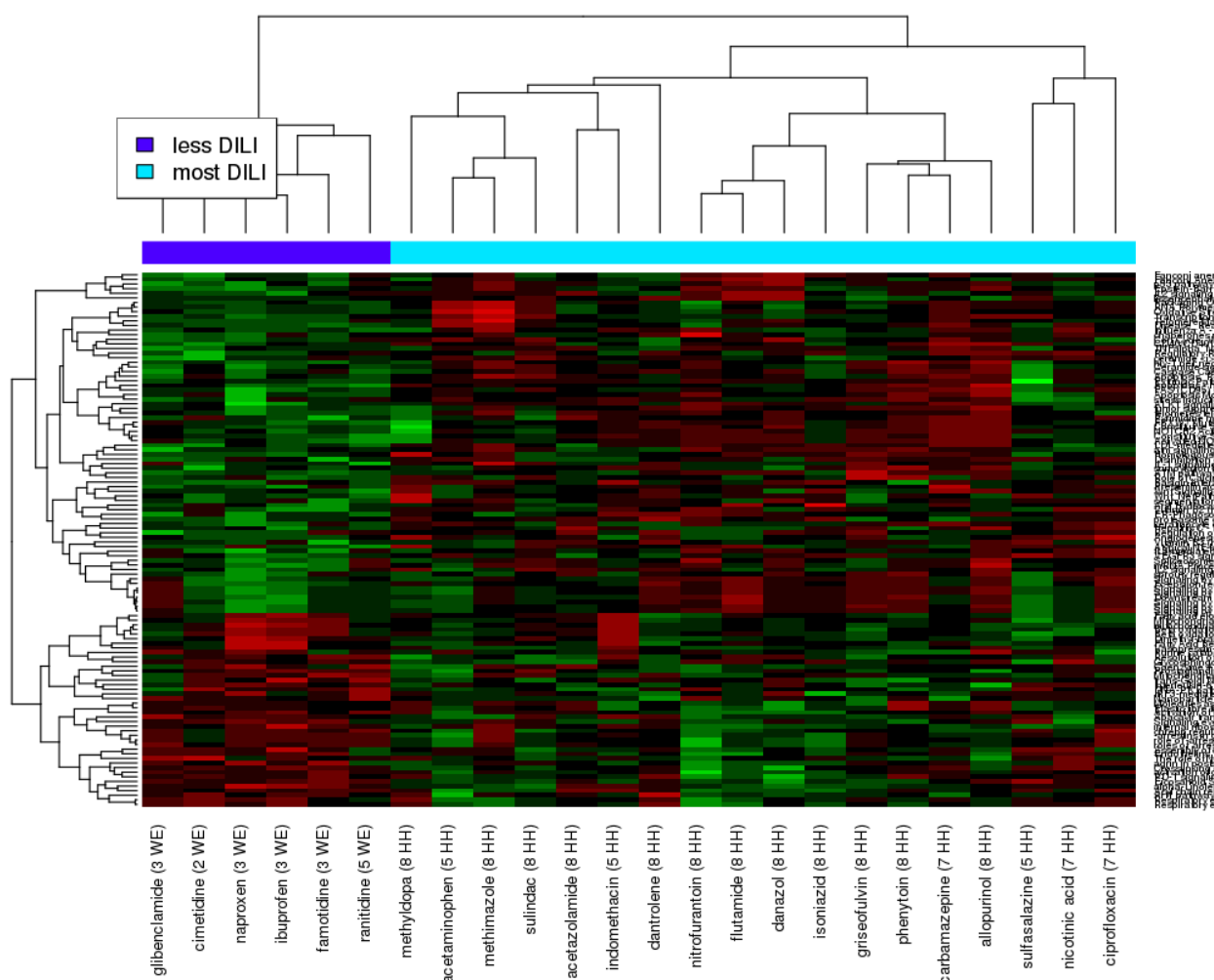


Figure 6: Hierarchical clustering of compounds based on the relative pathway response (RPR) scores for 115 pathways. Hierarchical clustering was done using complete-linkage as update rule and Pearson Correlation as pairwise similarity measure.

Clustering exhibits two main clusters of pathway response: an increase in response with respect to the severe DILI compounds and a loss in response with respect to the severe DILI compounds. On average the highest gain in response (Fig. 7) was due to Aryl Hydrocarbon Receptor (AHR) signalling (ca. 180% increase in response). This finding is consistent with literature knowledge since the aryl hydrocarbon receptor is known to be a ligand-dependent transcription factor that regulates the transcription of certain key enzymes involved in the metabolism of xenobiotic substances including drugs. The AHR can be activated by a wide range of classes of compounds (e.g. polycyclic aromatic hydrocarbons, benzimidazoles and flavonoids), and interacts with a number of other proteins, including nuclear hormone receptors. The cytochrome P450s CYP1A1, -1B1, -1A2 and -2S1 are regulated by the AHR, and they are all involved in the metabolism of endogenous substrates as well as xenobiotics.

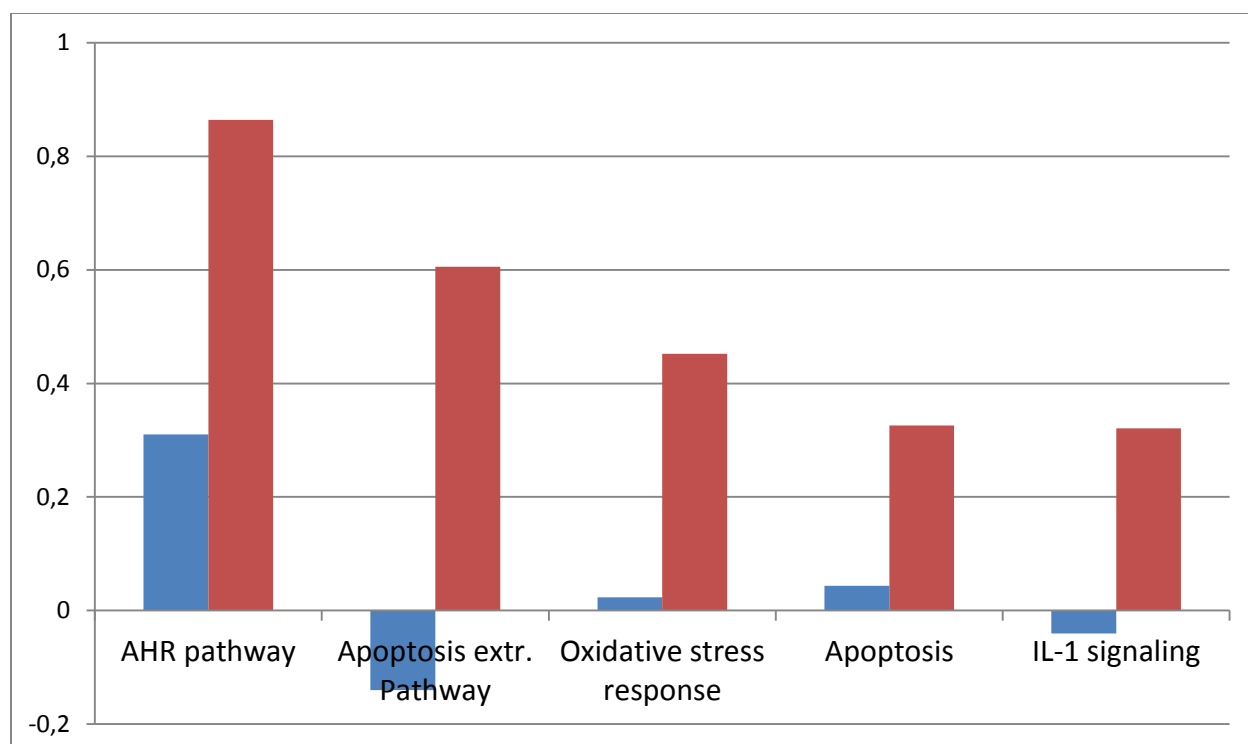


Figure 7: Gain in response of key DILI pathways. Blue bars: average relative pathway response scores with 'Less-DILI' compounds (n=6); red bars: average relative pathway response scores with 'Most-DILI' compounds (n=18).

We further used the 115 pathway profiles in order to classify the remaining seven compounds that were assigned 'Most-DILI' concern and that were not used for training because they lack DILI annotation in Greene et al. (cf. Fig. 4). Only one of these compounds was assigned to the wrong class (14%) while six of the compounds were assigned to the right class (86%) judged on pathway patterns. Using leaving-one-out cross validation with also the training compounds, all drugs were correctly classified. Performing the same classification procedure at the gene expression profiling level yields a correct prediction rate of only 65%.

We thus conclude that the toxicity classification at the pathway level outperforms the prediction at the gene level and that the derived pathway patterns are highly predictive of DILI. Although these results are encouraging and improve over existing prediction systems two critical points should be mentioned:

1. We used a relatively small subset of different compounds both for training (n=24) and for testing (n=7 novel compounds; n=31 resp. with cross-validation) so that the challenge remains to test these features with larger compound numbers when human *in vitro* microarray data becomes eventually available;
2. Annotation is critical. For example, there are several compounds that have conflicting results with the two classification systems under analysis. For these compounds the classification could not be made because they could not be assigned to either of the classes. However, there might be many different drugs that could not be uniquely annotated and solutions for these drugs are still pending.

To summarize we have designed a well-characterized training set of DILI compounds overlaying different annotation systems, performed pathway-level data analysis and identified 115 initial pathway concepts that are highly predictive of DILI risk (86%).

5. Repository with benchmark data (Milestone MS27)

In order to deliver to the consortium - and the interested community - the described pathway concepts along with benchmark gene expression data, MPIMG (in cooperation with UM) have developed a repository that contains the aggregated data.

5.1 Implementation and availability

The backend of the ToxDB is made up of a PostgreSQL database (version 9.2.4) running on an Apache/2.4.4 (64-bit Unix) server. The frontend HTML is designed using Flask (version 0.10.1), a web framework for Python (version 3.4.1). Pathway data is currently based on release 29 of the ConsensusPathDB. Most graphs are done with the help of JavaScript and the Google Visualization tools. The ToxDB will become freely available for the community under <http://toxdb.molgen.mpg.de> upon acceptance of the respective manuscript.

5.2 Drug view

From the start site of the ToxDB the user can select the drug view. Purpose of the drug view is to give a characterization of drug action at the pathway level. The user specifies a certain drug along with details on the experimental set up by selecting the organism, cell type, exposure time and dosage of the drug. The resulting page is displayed in Fig. 8. It shows a bar plot that presents the pathway scores along with the background distribution and the corresponding p-value that judges the significance of the response. A slider can be used to set the thresholds of the pathway scores with respect to the display. Each bar represents a pathway and is further clickable. By doing so the user is guided towards the gene-based view containing all genes that were assigned to the pathway along with results from the statistical test. Finally, chemical information of the drug is given with external links to chemical databases and resources of the project partners (ChEMBL) and outside the consortium.

As an example we have displayed the pathway response in human in vitro hepatocyte cells with high dose and long (1 day) exposure time with respect to valproic acid (Fig. 8A). On top of the resulting pathway responses we find 'fatty acid omega beta oxidation'. This is consistent with literature knowledge since valproic acid is known as a substrate for the fatty acid β -oxidation (FAO) pathway, which takes place primarily in mitochondria. The toxicity of valproate has long been considered to be due primarily to its interference with mitochondrial β -oxidation, in particular through its effects on enzymes of FAO and cofactors such as CoA and/or carnitine (Silva et al., 2008).

By clicking on the pathway bar the user opens the gene view (Fig. 8B). Here, each gene associated with the pathway is shown with its fold-change in the respective treatment experiment. Additional information about the significance of the fold-change is given with mouse over.

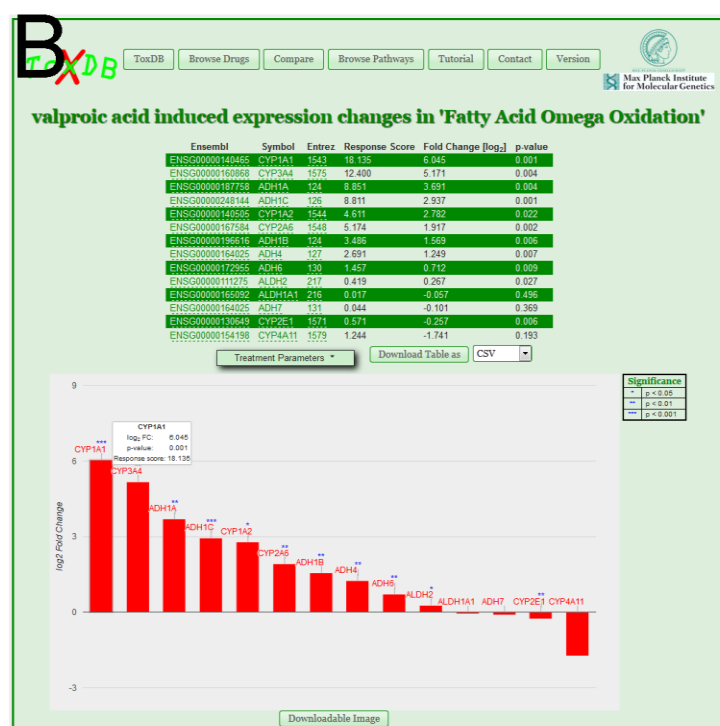
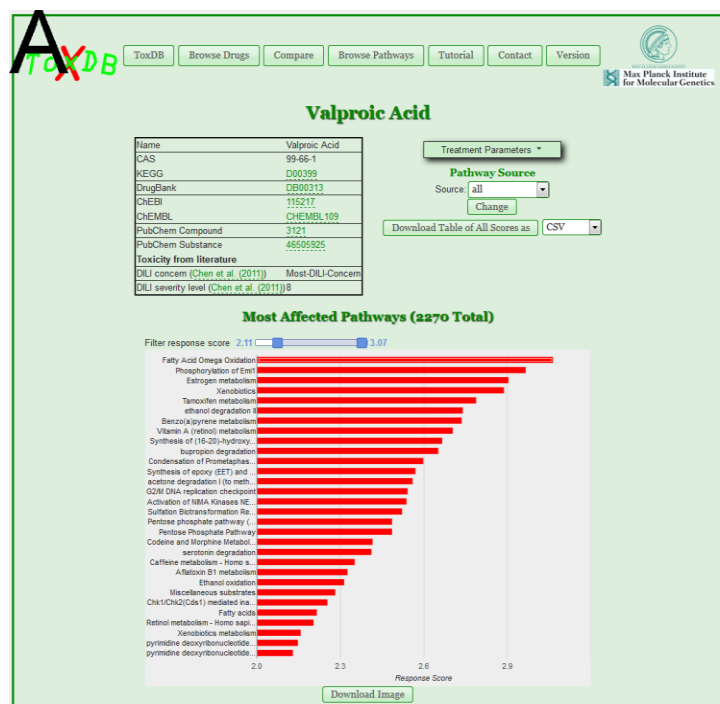


Figure 8 ToxDB drug view: A) After selecting the compound and the experimental setting under “Treatment parameters” the user gets the resulting pathway responses sorted after significance. A slider can be used to vary the number of displayed pathways. Chemical information can be retrieved with external links shown at the top left part of the page. B) By clicking on a specific pathway bar the gene view is opened. All genes assigned to the pathway are shown with their fold-change in the respective experiment.

5.3 Statistical testing

Commonalities and differences of *in vitro* vs. *in vivo* experiments, different organisms or different dosages and time points of drugs can be assessed with the testing functionality. It has been shown that relative pathway response scores are fairly Gaussian-distributed (Fig. 2A), thus, Student's t-test can be applied to judge whether two groups of experiments differ in their mean response. The ToxDB functionality takes advantage of these test results and allows the user to compare groups of experiments.

5.4 Pathway view

The pathway view functionality allows the user to retrieve information on a particular pathway, for example guided by a particular assay or validation experiment. Each experiment is shown with a bar plot indicating the response of the selected pathway in that experiment. As with the drug view, a slider can be used in order to vary the number of displayed features based on response score thresholds.

In order to assess the relevance of the pathway for toxicity, we included toxicity classification derived from two resources for the compounds. The first classification is based on the FDA assessment resulting in different DILI (drug-induced liver injury) severities ranging from negative DILI impact to severe phenotypes such as steatosis, cholestasis or acute liver failure (Chen et al., 2011). These severity scores were derived from extensive text mining and study of box warnings. The second classification is based on structure-activity relationships (SARs) and results in five classes of chemicals ranging from no evidence for toxicity (NE) to animal (AH) and human hepatotoxicity (HH; Greene et al., 2010).

As an example we used the pathway 'drug metabolism - cytochrome P450'. Clicking on it reveals the drug treatments that have the greatest effect on that pathway, i.e. those treatments that cause the highest expression changes in the genes involved in the pathway (Fig. 9). The top-scoring treatment (the left most bar in the chart) involves the drug rifampin applied to human *in vitro* liver cells at a dose of 2.8 μ M measured after 1 day. Study and treatment details can be viewed by hovering over the respective bar. The pathway response score of 4.3 is highly significant as indicated by far exceeding the three horizontal dashed lines in the plot with the background distribution. Those denote the 90%, 95%, and 99% quantiles, respectively, of the distribution of all pathway scores in the database. Furthermore, the treatments ranked 3rd and 10th also feature the drug rifampin at different dosages (14 μ M and 70 μ M, respectively).

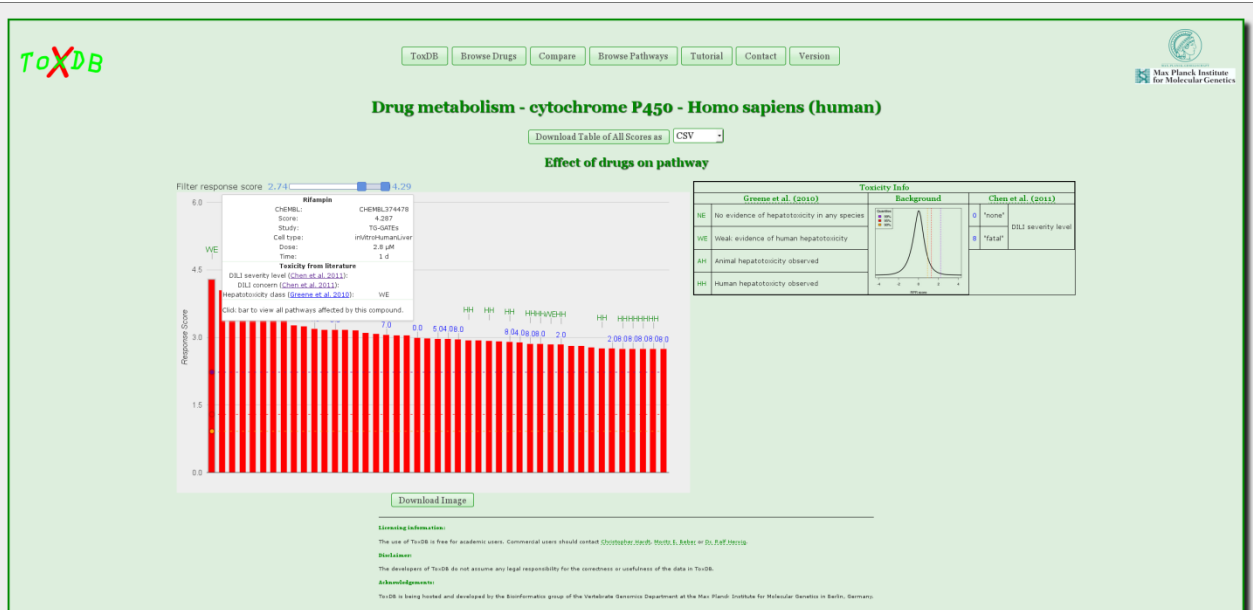


Figure 9: Pathway View of the KEGG representation of the cytochrome P450 pathway showing the most effective drug treatments.

Rifampin is used as a potent and broad spectrum antibiotic drug that is known to induce the xenobiotic cytochrome P450 pathway by increasing CYP3A4 activity. This particular effect is confirmed by the data in ToxDB, as can be seen when switching to the gene expression view of rifampin with respect to the pathway (Fig. 10). This view lists all genes involved in that pathway with their respective responses upon drug treatment. Here, clearly the most affected gene is CYP3A4 with a \log_2 fold change of 6.8 and a p-value of $1e-4$, followed by other members of the cytochrome P450 family (CYP2B6, CYP3A5, CYP2C8, CYP2C9, CYP2C19, and CYP2A6). Most of those have been shown to be induced by rifampin as well.

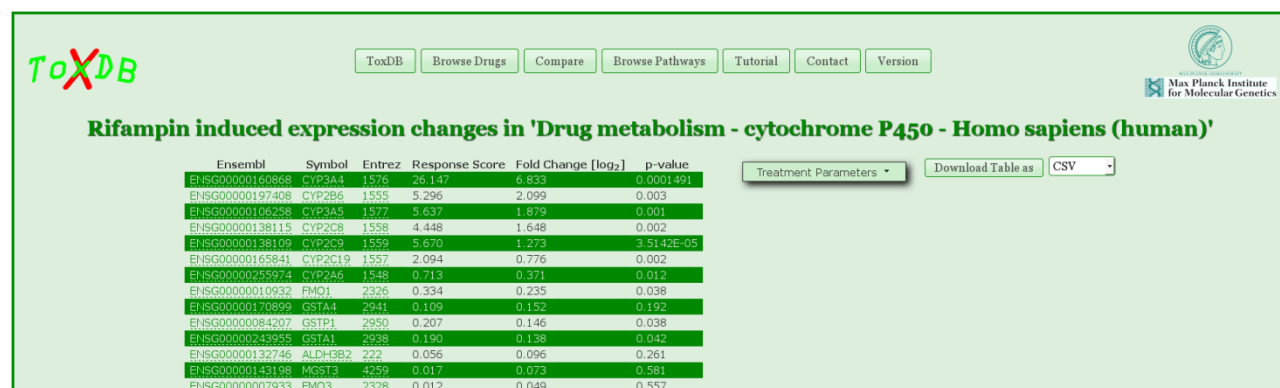


Figure 10: Gene Expression View of the KEGG representation of the cytochrome P450 pathway showing the most affected genes after upon treatment with the drug rifampin.

Rifampin is also believed to be hepatotoxic, i.e. promoting liver disease. When going to the DrugView of rifampin, setting the treatment parameters from above (study: TG-GATEs, celltype: InVitroHumanLiver, dose: 2.8 μ M, time: 1d) and setting the lower bound of the response scores to ~ 1.36 , some liver-related pathways show up: 'Fatty acid biosynthesis' and 'Fatty acid degradation'. Selecting other rifampin treatments reveal similar results.

As a second example we used the pathway 'non-alcoholic fatty liver disease' (NAFLD). NAFLD is described as being the most frequent cause of liver disease in the Western world. The KEGG representation of that pathway can be found in ToxDB and reveals drug treatments that have the highest impact on it (Fig. 11). The top-scoring treatment features the drug acarbose applied to rat hepatocytes (response score = 2.4,). Acarbose is commonly used to treat cardiovascular disease (CVD) in patients with type 2 diabetes.

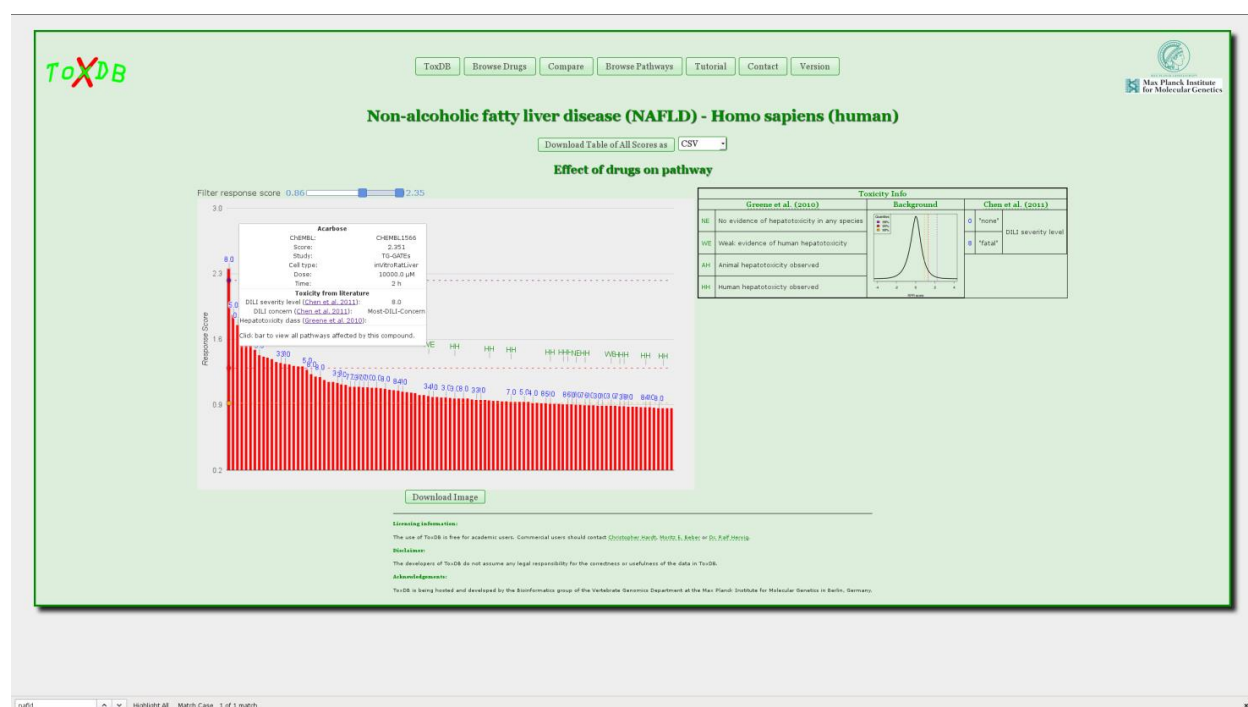


Figure 11: Pathway View of the KEGG representation of the NAFLD pathway showing the most effective drug treatments.

Chen et al. (2010) have classified many drugs with respect to their potential to cause drug-induced liver injury. Acarbose was considered as having 'most-DILI-concern' and given the highest severity class 8. This effect is reflected in the high pathway response in Fig. 11. Switching to the gene expression view allows for analysis of the pathway genes' individual responses (Fig. 12). Here, it can be seen that the interleukins IL1B, IL1A, and IL6 as well as tumor necrosis factor (TNF) show the greatest response. All four of them have been described as mediators of the inflammatory response.

acarbose induced expression changes in 'Non-alcoholic fatty liver disease (NAFLD) - Homo sapiens (human)'						Treatment Parameters		Download Table as	CSV
Ensembl	Symbol	Entrez	Response Score	Fold Change (log ₂)	p-value				
ENSG00000125538	IL1B	3553	13.441	5.670	0.00426				
ENSG00000115008	IL1A	3552	13.045	3.850	0.000409				
ENSG00000136244	IL6	3569	7.677	3.000	0.00276				
ENSG00000232810	TNF	7124	3.175	1.710	0.0139				
ENSG00000184557	SOC3	9021	0.705	0.467	0.031				
ENSG00000004779	NCUFA81	4706	0.481	0.393	0.0598				
ENSG00000155094	BR2211	10018	0.393	0.382	0.0926				
ENSG00000175327	MAP2K11	4256	0.130	0.346	0.423				
ENSG00000110717	NCUFS8	4738	0.254	0.265	0.169				
ENSG00000262077	MLXPL	51085	0.296	0.248	0.0641				
ENSG00000169429	IL8	3576	0.119	0.259	0.319				

Figure 12: Gene expression view of the KEGG representation of the non-alcoholic fatty liver disease (NAFLD) pathway showing the most affected genes after upon treatment with the drug acarbose.

These use cases demonstrate how ToxDB can be used to analyze specific, for example disease-related, pathways with respect to their susceptibility to a wide array of different drug treatments. The approach can help to identify drug treatments that enable certain pathways in order to deliberately combat malfunctions or diseases. Furthermore, it may identify drugs that promote or facilitate a particular disease of interest, in which case it may be advisable to switch to an alternative treatment (drug and/or dose) with a lesser effect on the corresponding pathway.

SUMMARY

MPIMG explored a pathway-based toxicogenomics approach. This approach consists of *i)* mapping of toxicogenomics data on pathways (rather than on single genes), *ii)* deriving a weighted pathway interaction graph, and *iii)* computing of network modules on the pathway interaction graph in order to identify molecular themes (i.e. sets of interacting pathways) that are most responsive with respect to the compound under study. This approach was conducted for 1,152 multiple time-dosage drug experiments and in particular investigated in a subset of 119 drug experiments in human in vitro hepatocytes and 72 drug experiments in rat in vivo heart tissue. Furthermore, a well-characterized subset of 61 drug experiments from the first data set was used for testing the capability of DILI hazard prediction. In all three studies we showed that pathway-based analysis of toxicogenomics data prioritized molecular themes that are predominantly associated with liver and heart toxicity, in particular dysfunction of mitochondria and, thus, that this approach can be used to guide future molecular models (**WP2**) and construction and refinement of AOPs (**WP11**) to be developed in HeCaToS.

DIFFICULTIES

We experienced a delay of four months mainly because of the underestimated complexity of the tasks. For example, deriving a pathway scoring (which was initially done at single experiments, i.e. a single time point and a single dose regimen as published by Yildirimman et al., 2011) from time-dose variations was not straightforward and several different models of the data had to be implemented and tested. Furthermore, the design and implementation of the ToxDB interface and the practical testing took more time than expected.

REFERENCES

- Hendrickx DM, Aerts HJ, Caiment F, Clark D, Ebbels TM, Evelo CT, Gmuender H, Hebels DG, Herwig R, Hescheler J, Jennen DG, Jetten MJ, Kanterakis S, Keun HC, Matser V, Overington JP, Pilicheva E, Sarkans U, Segura-Lepe MP, Sotiriadou I, Wittenberger T, Wittwehr C, Zanzi A, Kleinjans JC. (2015) diXa: a data infrastructure for chemical safety assessment. *Bioinformatics*. 31(9):1505-7.
- Herwig R. (2014) Computational modelling of drug response with application to neuroscience. *Dialogues Clin Neurosci*, 16(4):465-77.
- Hebels DG, Jetten MJ, Aerts HJ, Herwig R, Theunissen DH, Gaj S, van Delft JH, Kleinjans JC (2014) Evaluation of database-derived pathway development for enabling biomarker discovery for hepatotoxicity. *Biomark Med*, 8:185-200.
- Kamburov A, Stelzl U, Lehrach H, Herwig R (2013) The ConsensusPathDB interaction database: 2013 update. *Nucleic Acids Res*, 41:D793-D800.
- Kamburov A, Grossmann A, Herwig R, Stelzl U (2012) Cluster-based assessment of protein-protein interaction confidence. *BMC Bioinformatics*, 13:262.
- Kamburov A, Stelzl U, Herwig R (2012) IntScore: a web tool for confidence scoring of biological interactions. *Nucleic Acids Research*, 40:W140-W146.

ANNEX 1: 119 COMPOUNDS ANALYSED IN HUMAN *IN VITRO* HEPATOCYTES FROM TG-GATES

phenylbutazone	chlormadinone	haloperidol
simvastatin	bucetin	ethanol
colchicine	theophylline	mexiletine
carbamazepine	papaverine	griseofulvin
valproic acid	nifedipine	nimesulide
lornoxiam	acetazolamide	clofibrate
imipramine	ethionine	nitrofurantoin
acetaminophen	hexachlorobenzene	nicotinic acid
caffeine	diltiazem	enalapril
pemoline	benziodarone	meloxicam
diazepam	allyl alcohol	indomethacin
erythromycin ethylsuccinate	phenylanthranilic acid	amitriptyline
chlormezanone	aspirin	amiodarone
dantrolene	sulpiride	isoniazid
chloramphenicol	WY-14643	promethazine
tiopronin	cimetidine	triazolam
naphthyl isothiocyanate	acetamidofluorene	fenofibrate
diclofenac	furosemide	mefenamic acid
methyltestosterone	rifampicin	ethinylestradiol
methapyrilene	thioacetamide	chlorpromazine
penicillamine	benzbromarone	fluphenazine
metformin	phenobarbital	ketoconazole
tetracycline	clomipramine	perhexiline
ethionamide	sulfasalazine	tolbutamide
allopurinol	labetalol	ciprofloxacin
danazol	etoposide	flutamide
omeprazole	carbon tetrachloride	terbinafine
methimazole	ethambutol	tamoxifen
propylthiouracil	gemfibrozil	ticlopidine
naproxen	methyldopa	ajmaline
azathioprine	glibenclamide	nitrofurazone
captopril	thioridazine	cyclophosphamide
acarbose	chlorpropamide	hydroxyzine
sulindac	chlorpheniramine	famotidine
moxisylyte	tannic acid	iproniazid
phenytoin	ranitidine	tacrine
bromobenzene	lomustine	disulfiram
phenacetin	disopyramide	quinidine
adapin	ibuprofen	vitamin A
nitrosodiethylamine	monocrotaline	

ANNEX 2: 72 COMPOUNDS ANALYSED IN RAT VIVO HEART TISSUE FROM DRUGMATRIX

candesartan	sirolimus
ifosfamide	isoprenaline
valsartan	cyclosporin A
valproic acid	buspirone
idarubicin	paroxetine
dicyclomine	chlorpropamide
celecoxib	chlorambucil
benzethonium chloride	azaribine
fludrocortisone	cyproheptadine
dexchlorpheniramine	doxorubicin
phenylephrine	haloperidol
rofecoxib	poly(allylamine hydrochloride)
oxybutynin	mitoxantrone
4'-epidoxorubicin	indomethacin
metoprolol	vinorelbine
spironolactone	pentoxifylline
noradrenaline	amiodarone
sulindac	clofibric acid
Vinblastine	trimethadione
phenytoin	acrolein
chlorobenzene	guanethidine
fexofenadine	risperidone
cisapride	valdecoxib
daunorubicin	etidronic acid
losartan	cyclophosphamide
1,4-dichlorobenzene	famotidine
angiotensin II	dobutamine
atenolol	gabapentin
acetylsalicylic acid	imatinib
sulpiride	fenofibrate
bezafibrate	fluocinolone acetonide
(S)-(-)-sulpiride	desloratadine
tacrolimus hydrate	
aldosterone	
furan	
flunarizine	
2'-beta-fluoro-2',3'-deoxyadenosine	
dexamethasone	
hydrocortisone	
fluoxetine	